The Retention Behavior of Reversed-Phase HPLC Columns with 100% Aqueous Mobile Phase

The authors studied the retention behavior of reversed-phase high performance liquid chromatography (HPLC) columns under 100% aqueous mobile-phase conditions. They report about the behaviors of reversed-phase HPLC columns such as C18 and C8 columns and discuss why they exhibit decreased retention times. They also suggest criteria for achieving reproducible results from reversed-phased columns under highly aqueous mobile-phase conditions.

Norikazu Nagae, Toshiyuki Enami, and Sid Doshi*
Nomura Chemical Co., Ltd., 851 Anada-cho, Seto, 489-0003, Japan
* Phenomenex, 2320 West 205th Street, Torrance, California 90501-1456

Address correspondence to N. Nagae.

Octadecyl (C18) and octyl (C8) are the most widely used bonded phases in reversed-phase high performance liquid chromatography (HPLC). However, C18 and C8 reversed phases also exhibit decreased and poorly reproducible retention under more than 98% aqueous conditions. This problem traditionally has been explained as being the result of ligand collapse or a matting effect. Wolcott and Dolan (1) reported that when a C18 column was washed with water, the bonded phase collapsed. Subsequent flushing with mobile phase removed the wash solvent, but the stationary phase remained in the collapsed configuration, which caused a change in retention and selectivity. They advised that washing a reversed-phase HPLC column with water should be avoided. Furthermore, if the organic solvent content of a mobile phase was too low, the stationary phase would tend to collapse onto itself in a low-energy conformation. This collapse could lead to abnormal chromatographic behavior and generally undesirable results. To avoid this phenomenon, scientists recently have used embedded polar phases, including amide or carbamate groups (2–5), which supposedly do not undergo phase collapse in 100% water. These stationary phases' higher polarity limits their applicability in HPLC because they show shorter retention and stability in reversed-phase liquid chromatography (LC).

In our work, we studied retention behavior under 100% aqueous mobile-phase conditions for several reversed phases such as trimethylsilyl silica, C8, C18, and triacontylsilyl silica (C30). When the pore size of the silica supports was larger, some phases showed the decreased retention times, but others had higher reproducibility in retention. Through this process, we discovered new information about the real mechanism causing the decrease in retention under 100% aqueous mobile-phase conditions (6,7). We found that standard C18 reversed-phase columns could provide reproducible results under 100% aqueous mobile-phase conditions as long as they met certain criteria.

Experimental

Apparatus: The LC system comprised a model PU-980 pump, a model UV-980 UV detector, and a model 830-RI refractive index detector (all from Jasco, Tokyo, Japan); a model 7725 injector (Rheodyne, Rohnert Park, California); and a model SIC 480 integrator (System Instrument, Tokyo, Japan). We controlled the column temperature between 30 and 80 °C using a water bath and a heater with a model E5C3 temperature controller (Omron, Tokyo, Japan) and between 5 and 30 °C using a heater and

Table I: Characteristics of the stationary phases examined in this work*

Stationary Phase	Specific Surface Area (m^2/g)	Pore Volume (mL/g)	Mean Pore Diameter (nm)	Carbon Content (%)	Ligand Density ($\mu mol/m^2$)
Trimethylsilyl silica	223	0.93	12.9	4.7	4.8
Trimethylsilyl silica	302	0.91	9.3	5.0	4.3
Trimethylsilyl silica	331	0.65	6.5	6.3	4.1
C8	128	0.90	22.4	5.6	3.1
C8	142	0.88	19.0	7.2	3.3
C8	169	0.84	15.1	8.4	3.1
C8	199	0.74	11.3	10.6	3.3
C18	113	0.80	21.9	11.4	3.4
C18	123	0.73	17.9	12.8	3.2
C18	139	0.65	13.9	13.9	3.0
C18	163	0.58	10.4	18.4	3.2
C30	176	0.60	10.4	18.0	1.8
C30	219	0.53	7.2	19.7	1.2
C30	210	0.43	6.2	21.2	1.0

*All measurements were performed on bonded phases.

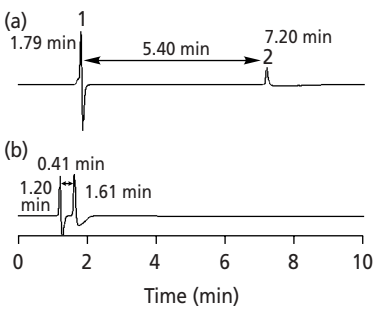

Figure 1: Retention behavior of a C18 column under 100% aqueous mobile-phase conditions. Shown are (a) initial results and (b) results after stopping the pump for 1 h and then starting it again. Column: 150 mm × 4.6 mm, 5-μm d_p C18, 10-nm pore size; mobile phase: water; flow rate: 1.0 mL/min; column pressure: 6.0 MPa; temperature: 40 °C; detection: refractive index; added back pressure: 1.7 MPa after the column. Peaks: 1 = sodium nitrate (t_0), 2 = 2-propanol.

Table II: Retention time and weight of a C18 column under 100% aqueous mobile-phase conditions

	t_0 (min or mL)	$t_{2\text{-propanol}}$ (min or mL)	$t_{2\text{-propanol}} - t_0$ (min or mL)	%	Mass of Column (g)
Initial	1.79	7.20	5.41	100	62.0
After stopping	1.20	1.61	0.41	7.6	61.4
Initial − after	0.59	5.59	5.00	92.4	0.6

a cooler (Orion Kikai, Tokyo, Japan). The particle size, pore size, and surface area measurements were obtained using Coulter Multisizer and Coulter SA-3100 instruments (both from Beckman Coulter, Fullerton, California). The carbon load was determined using a CN-corder MT-700 instrument (Yanaco, Kyoto, Japan).

Reagents and chemicals: We prepared distilled water in the laboratory. Other solvents and buffer constituents were purchased from Wako (Osaka, Japan). The tested solutes also were from Wako. Table I lists the stationary phases used in our study.

Trimethylsilyl silica, C8, C18, and C30 phases were generated using trimethylchlorosilane, dimethyloctylchlorosilane, dimethyloctadecylchlorosilane (all from Shin-etsu Silicon Chemicals, Tokyo, Japan), and dimethyltriacontylchlorosilane (Gelest, Tullytown, Pennsylvania) by the conventional refluxing method in toluene for 12–48 h with pyridine and excess reagent. All phases, except for trimethylsilyl silica, were bonded with trimethylchlorosilane twice by the same manner as the above as an endcapping. The hydrogen-bonding capacity, which was the separation factor of caffeine and phenol obtained using 75:25 (v/v) methanol–water as a mobile phase, was less than 0.6 on all phases. The silica gel used in bonding was from Nomura Chemical (Seto, Japan).

Table I also lists the characteristics of the stationary phases. The bonded phases were slurry packed with chloroform into a 150 mm × 4.6 mm column blank (Sugiyama Shoji, Yokohama, Japan).

Results and Discussion

It is well known that the retention time of a C18 phase is reduced under 100% aqueous mobile-phase conditions. Figure 1 shows the change of retention time of sodium nitrite and 2-propanol on a 10-nm pore size C18 phase at 40 °C. We used the sodium nitrite to measure the unretained time (t_0). We added back pressure to the column when the mobile phase was changed to water — we will explain the reason for this change below. Stopping the flow for 1 h caused shorter retention times for both sodium nitrite and 2-propanol. The difference of retention time between sodium nitrite and 2-propanol became the essential retention of 2-propanol in this case. After no flow for 1 h, not only did the t_0 decrease from 1.79 min to 1.20 min, the essential retention of 2-propanol was only 7.6% compared with its initial retention. Generally, a decrease of t_0 is unexpected because t_0 is the unretained time.

We measured the column weight at the same time. The column was sealed at both ends with plugs as soon as the column pressure was reduced to 0 MPa. The decreases in t_0 and the column weight were 0.59 mL and 0.6 g, respectively, as Table II lists. The values were almost the same because the specific gravity of water is 1.0 g/mL. Furthermore, we observed that 0.6 mL of water went out of the outlet of the column during the 1 h when no mobile phase flowed through the column.

Figure 2 shows the effect of the pore size. We evaluated the retention behavior of 10- and 22-nm pore size C18 silica. The 10-nm C18 silica showed decreased retention times of thymine and sodium nitrite as t_0; however, the retention times of both sodium nitrite and thymine were unchanged on the 22-nm C18 silica. The only difference between these two C18 silicas is pore size. The larger pore size provided higher reproducibility in retention time under 100% aqueous conditions. From these results we ascertained that the mobile phase was being expelled from the pores of the packing material under 100% aqueous mobile-phase conditions, as Figure 3 shows.

Figure 4 illustrates the relationship between the pore size and the relative retention time. The relative retention time was the ratio of the retention time after no flow for 1 h to the initial retention time at 40 °C. When comparing packing materials of the same pore size — at 15 nm and 6 nm, for example — a C8 phase showed the greatest decrease in retention, and the C30 phase showed the least decrease in retention. The longer the length of ligand, the smaller the decrease in retention, except for the trimethylsilyl ligand.

The trimethylsilyl ligand is so small that it influences the polarity of the silica surface. In other words, trimethylsilyl silica is more polar than the other phases compared in our study, and it is this polarity of the trimethylsilyl silica that likely influences the pore size shift to the small area. As we will discuss below, residual silanol groups showed a similar effect on the results. Furthermore, the trimethylsilyl phase did not appear to suffer phase collapse because it was a very short ligand. Trimethylsilyl phase bonded to a 6-nm pore size silica, however, did show a decrease in retention time.

On the other hand, the C18 ligand can collapse because of its long alkyl chain. We expect that the ligand of the 10- and 22-nm pore size C18 silica could collapse similarly under 100% aqueous conditions. Although the 10-nm C18 silica showed an 80% decrease in retention time, the 22-nm C18 silica exhibited less than a 5% decrease in retention time, as shown in Figure 4.

Other phases also showed similar results, although we evaluated many pore sizes. We can assume from these findings that phase collapse has nothing to do with the decrease in retention time on reversed-phase HPLC columns when used under 100% aqueous mobile-phase conditions.

Figures 5 and 6 show the effect of temperature on 10-nm pore size C18 and C30 phases. The C18 phase showed an 80% decrease in retention time at 40 °C; however, it showed an 8% decrease in retention time at 5 °C. The lower the temperature, the smaller the decrease in retention time. Even when the pump was running and pressure existed in the column, the retention time was reduced at more than 30 °C. On the other hand, the C30 phase showed a 20% decrease in retention time at 80 °C and 5% at 40 °C. The retention behavior of the C30 phase at 80 °C and at 40 °C is very similar to that of the C18 phase at 40 °C and 5 °C.

The melting points of octadecane ($C_{18}H_{38}$) and triacontane ($C_{30}H_{62}$) are 29–30 °C and 68–69 °C, respectively. It seems that retention behavior of the C18 and C30 phases is related to their respective melting points. Recently, Doyle and coworkers (8) reported the characterization of C18-bonded stationary phase by Raman spectroscopy. They concluded that bonded ligands did not exhibit the same phase-transition behavior as neat octadecane. The octadecane melted at a discrete temperature (28–30 °C); the spectral features of the C18 ligands, which more closely resemble those of liquid than solid octadecane, gradually and continually varied with changes in temperature throughout the 2–45 °C range investigated.

The change of retention behavior in Figure 5 was gradual and continual — not a sudden phase transition. An end of the C18 ligand was bonded on the surface of the silica gel, so that the behavior of C18 ligands naturally was different from that of neat octadecane. The temperature range with changes of C30 ligands was higher than that

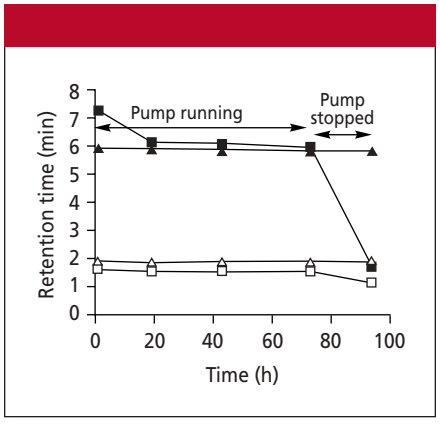

Figure 2: Effect of the pore size on retention under 100% aqueous mobile-phase conditions. Column: 150 mm × 4.6 mm, 5-μm d_p C18, 10-nm pore size; mobile phase: 10 mM phosphate buffer (pH 7.0); flow rate: 1.0 mL/min; column pressure: 6.0 MPa; temperature: 40 °C; detection: UV at 254 nm. Sample: □ = C18 (10-nm pore size) — sodium nitrite, △ = C18 (22-nm pore size) — sodium nitrite, ■ = C18 (10-nm pore size) — thymine, ▲ = C18 (22-nm pore size) — thymine.

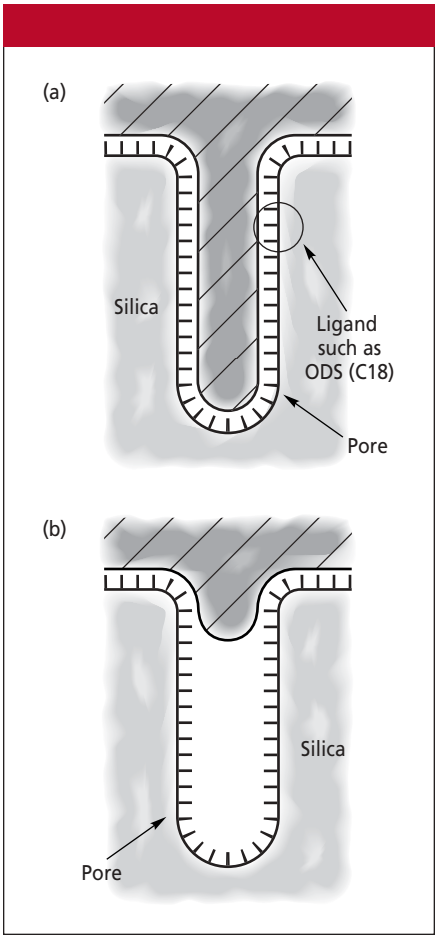

Figure 3: Behavior of (a) an organic solvent–water mobile phase, which fills the silica gel pore, and (b) water mobile phase, which is expelled from the pore.

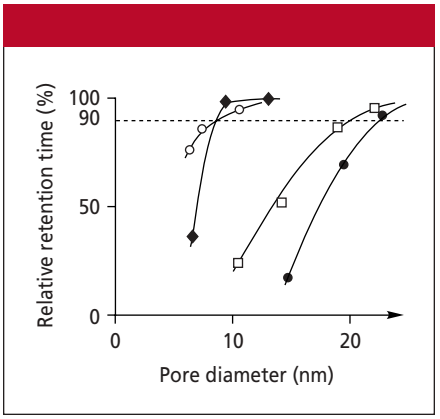

Figure 4: Relationship between pore size and relative retention time with 100% aqueous mobile phase. Column: C30 (○), C18 (□), C8 (●), and trimethylsilyl silica (◆); column dimensions: 150 mm × 4.6 mm; sample: thymine. Other conditions were the same as in Figure 2. Relative retention time was calculated as the ratio of the decrease in retention versus initial retention time.

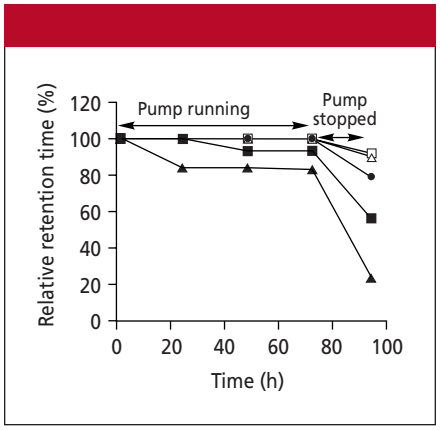

Figure 5: Effect of temperature on C18 column (10-nm pore size) under 100% aqueous mobile-phase conditions. Column dimensions: 150 mm × 4.6 mm; temperature: □ = 5 °C, △ = 10 °C, ● = 20 °C, ■ = 30 °C, ▲ = 40 °C. Other conditions were the same as in Figure 4.

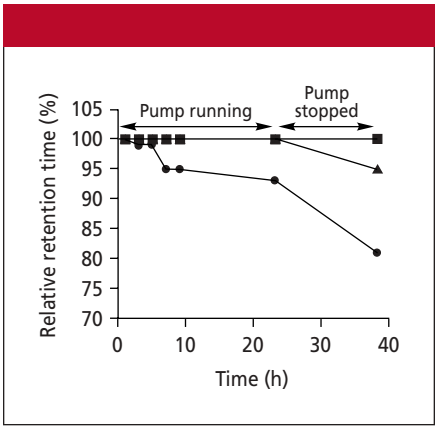

Figure 6: Effect of temperature on C30 (10-nm pore size) under 100% aqueous mobile-phase conditions. Column dimensions: 150 mm × 4.6 mm; temperature: ■ = 30 °C, ▲ = 40 °C, ● = 80 °C. Other conditions were the same as in Figure 4.

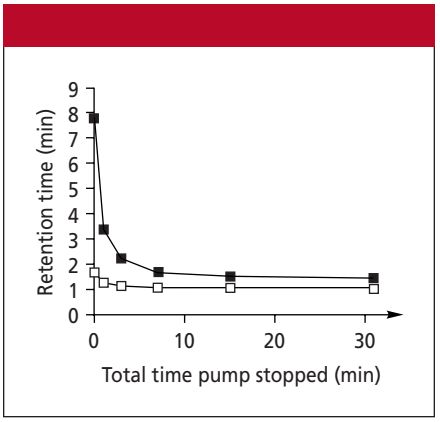

Figure 7: Effect of stopping flow. Column: 150 mm × 4.6 mm C18, 10-nm pore size. Sample: □ = sodium nitrite, ■ = thymine. Other conditions were the same as in Figure 4.

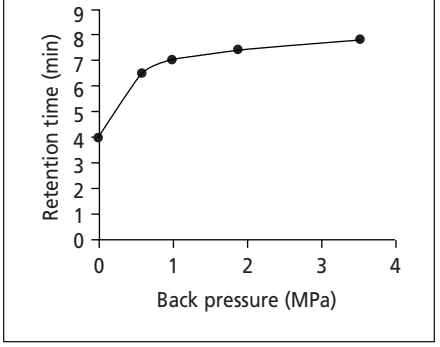

Figure 8: Effect of back pressure. Column: 150 mm × 4.6 mm 20-μm d_p C18, 10-nm pore size; column pressure: 0.4 MPa; sample: thymine. Other conditions were the same as in Figure 4. Resistance was added after the column.

of C18 ligands by 40 °C. We assumed that when the temperature was higher than the melting point of the ligand, the degree of freedom for movement for each ligand became high, so we see that the mobile phase is easily expelled from the pore. This change explains why the C8 phase showed the greatest decrease in retention time in Figure 4 — because the melting point of octane (C_8H_{18}) is lower than that of octadecane.

Figures 7 and 8 show the effect of stopping flow and back pressure after the column. The decrease in retention time was finished in several minutes at 40 °C, as shown in Figure 7. This result shows that the mobile phase immediately went out of a column at 40 °C when no pressure was in the column. The particle size of packing materials tested in Figure 8 was 20 μm, and the column pressure was 0.4 MPa. When adding back pressure after the column, the pressure on the inlet of the column was 0.4 MPa in addition to its back pressure. When the pressure was greater than 3.6 MPa around the packing materials, the retention time was 7.8 min, as shown in Figure 8. However, when less than 0.4 MPa of pressure existed around the packing materials, the retention time was 4 min.

In other words, 20-μm d_p, 10-nm pore size octadecylsilyl silica showed a decrease in retention time from the beginning without the back pressure because the pressure around the packing materials was insufficient for the mobile phase to remain in the pores of the packing materials. Even if the column was packed with 5-μm d_p packing materials and the column pressure was high, we found that the mobile phase was expelled from the pore of the packing materials near the outlet of the column, as shown in Figure 9, because of very low pressure near the outlet. A 1.7-MPa postcolumn back pressure caused the retention time of 2-propanol to increase from 6.5 min to 7.2 min. This back pressure also is considered to be a factor responsible for lowering reproducibility in retention. Therefore, the back pressure after the column makes reproducibility in retention high.

Table III documents the effect of endcapping for three types of C18 columns (Develosil by Nomura Chemical). One column was not endcapped, and the others were single- and double-endcapped with trimethylchlorosilane. All were used to evalu-

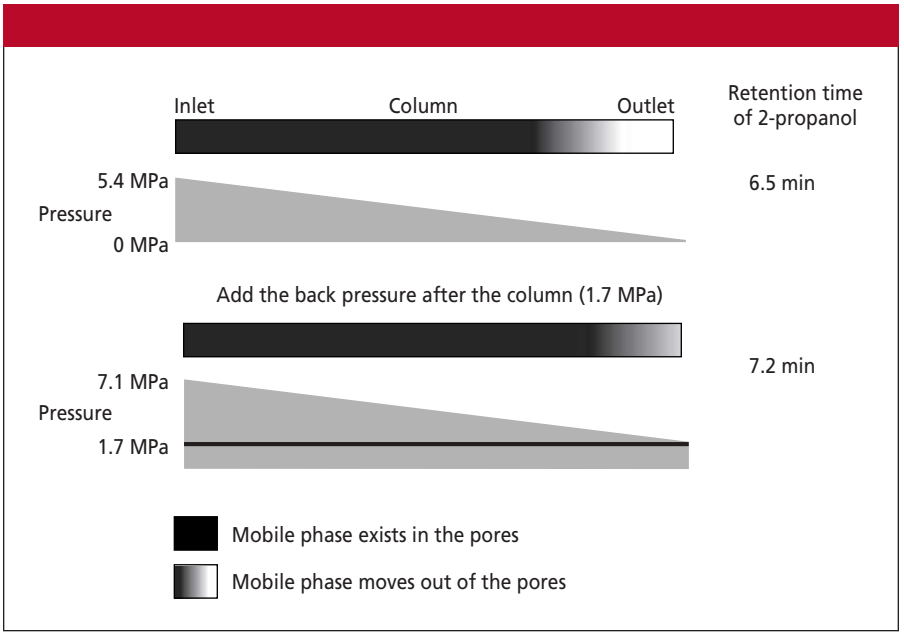

Figure 9: State of the packing material in the column. Conditions were the same as in Figure 1.

Table III: Effect of endcapping*

Column	Endcapping	Hydrogen-Bonding Capacity†	Relative Amount of Residual Silanol Groups	Final Retention Time Ratio‡ (%)
Develosil ODS-A-5	No	1.42	Much	97.5
Develosil ODS-T-5	Single	0.53	Little	58.2
Develosil ODS-HG-5	Double	0.38	Very little	39.9

*Conditions as shown in Figure 4.
†Hydrogen-bonding capacity: separation factor of caffeine and phenol.
‡The final retention time ratio is the final retention when the retention time decreased to the initial retention time.

ate the effect of the residual silanol groups. We measured the amount of residual silanol groups on the bonded phase by evaluating their hydrogen-bonding capacity. The higher the hydrogen-bonding capacity, the greater the number of residual silanol groups. More extensive endcapping reduced the amount of residual silanol groups and thereby caused poor reproducibility in retention time, as shown in Table III. The residual silanol groups work as polar groups on the stationary phase. The polarity of stationary phases with high residual silanol group content is high, so these phases show high reproducibility in retention much as do embedded polar phases such as alkylamide and alkylcarbamate phases.

Similarly, trimethylsilyl silica has high hydrogen-bonding capacity and is more polar than a C8 phase, hence a trimethylsilyl silica phase with a 9-nm pore size displays high reproducibility in retention, as shown in Figure 4. A C18 phase without endcapping is very unstable especially under neutral pH and highly aqueous conditions because of the existence of these silanol groups. Therefore, this type of C18 column cannot be used.

Figures 10 and 11 illustrate the effect of salt and ion-pair reagents. The relative retention largely was influenced by the concentration of salt and ion-pairing reagent, as these figures show. Only 5 mM of ion-pairing reagent showed very high reproducibility in retention. We think that the salt and ion-pairing reagent decreased the surface tension of the mobile phase while simultaneously making the stationary phase more hydrophilic. With this low surface tension, the highly hydrophilic stationary phase easily could keep the mobile phase in the pore.

After the aqueous mobile phase was expelled from the pore of the packing materials, we eluted the mobile phase with a greater than 50% concentration of organic solvent to return the mobile phase into the pore. We flushed the column with 70:30 (v/v) acetonitrile–water at the end of each evaluation, and the column always returned to its initial state. We repeated the experiment several times using the same column, and we obtained the same results each time.

Conclusion

We have confirmed that reversed-phase HPLC columns show a decrease in retention under 100% aqueous conditions because under these conditions the mobile phase is expelled from the pore of the packing materials, which results in decreased contact between the stationary and mobile phases. Some critical parameters — such as pore size, the length of the alkyl group bonded to the stationary phase, temperature, pressure, endcapping, and the concentration of salt and the ion-pairing reagent — influence the decrease in retention. When the pore size of packing materials is greater than 22 nm and the operating temperature is lower than 10 °C or 5 mM of ion-pairing reagent is added to the mobile phase, even a common C18 HPLC column shows high retention reproducibility under 100% aqueous conditions.

We also found that a 10-nm pore size C30 phase used at temperatures lower than 40 °C showed high retention reproducibility without any of the above conditions, thereby making it an ideal phase to use for highly aqueous mobile-phase applications (9).

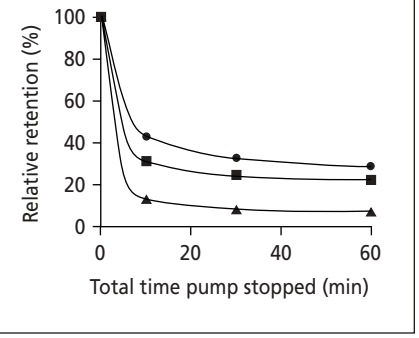

Figure 10: Effect of concentration of salt in the mobile phase. Column: 150 mm × 4.6 mm C18, 10-nm pore size; mobile phase: ▲ = water, ■ = 10 mM ammonium phosphate (pH 7.0), ● = 100 mM ammonium phosphate (pH 7.0). Other conditions were the same as in Figure 1.

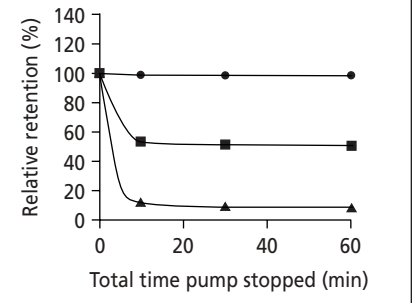

Figure 11: Effect of the concentration of the ion-pairing reagent. Column: 150 mm × 4.6 mm C18, 10-nm pore size; mobile phase: ▲ = 10 mM sodium phosphate (pH 7.0), ■ = 10 mM sodium phosphate–1 mM sodium octanesulfonate (pH 7.0), ● = 10 mM sodium phosphate–5 mM sodium octanesulfonate (pH 7.0). Other conditions were the same as in Figure 1.

References

(1) R.G. Wolcott and J.W. Dolan, *LCGC* **17**(4), 316–321 (1999).
(2) J.E. O'Gara, B.A. Alden, T.H. Walter, J.S. Petersen, C.L. Niederlander, and U.D. Neue, *Anal. Chem.* **67,** 3809–3813 (1995).
(3) T. Czajkowaka, I. Hrabovsky, B. Buszewski, R.K. Gilpin, and M. Jaronieic, *J. Chromatogr. A* **691,** 217–224 (1995).
(4) T.L. Ascah, K.M.R. Kallury, C.A. Szafravski, S.D. Corman, and F. Liu, *J. Liq. Chromatogr. Rel. Technol.* **19,** 3409–3073 (1996).
(5) T. Czajkowaka and M. Jaronieic, *J. Chromatogr. A* **762,** 147–158 (1997).
(6) N. Nagae and T. Enami, *Bunseki Kagaku* **49,** 887–893 (2000).
(7) T. Enami and N. Nagae, *Chromatography* **22,** 33–39 (2001).
(8) C.A. Doyle, T.J. Vickers, C.K. Mann, and J.G. Dorsey, *J. Chromatogr. A* **877,** 41–59 (2000).
(9) N. Nagae, Nomura Chemical Co., Ltd., U.S. patent number 6,241,891, 5 June 2001. ■